

1 A 406-year non-growing season precipitation reconstruction in the 2 southeastern Tibetan Plateau

3 Maierdang Keyimu^{1,2}, Zongshan Li^{1*}, Bojie Fu¹, Guohua Liu¹, Weiliang Chen¹, Zexin ~~Fan~~²Fan³, Keyan
4 ~~Fang~~³Fang⁴, Xiuchen ~~Wu~~⁴Wu⁵, Xiaochun ~~Wang~~⁵Wang⁶

5 ¹State Key Laboratory of Urban and Regional Ecology, Research Center for Eco-Environmental Sciences, Chinese Academy
6 of Sciences, Beijing 100085, China

7 ²Xinjiang Key Laboratory of Desert Plant Roots Ecology and Vegetation Restoration, Xinjiang Institute of Ecology and
8 Geography, Chinese Academy of Sciences, Urumqi 830011, China

9 ³Xishuangbanna-³Xishuangbanna Tropical Botanical Garden, Chinese Academy of Sciences, Mengla 666303, China

10 ³~~Key~~-⁴Key Laboratory of Humid Subtropical Eco-Geographical Process (Ministry of Education), College of Geographical
11 Sciences, Fujian Normal University, Fuzhou 350007, China

12 ⁴~~State~~-⁵State Key Laboratory of Earth Surface Processes and Resource Ecology, Beijing Normal University, Beijing 100875,
13 China

14 ⁵~~College~~-⁶College of Forestry, Northeast Forestry University, Harbin 150040, China

15 *Correspondence to:* Zongshan Li (zqli_st@rcees.ac.cn)

16 **Abstract.** Trees record climatic conditions during their growth, and tree rings serve as proxy to reveal the features of the
17 historical climate of a region. In this study, we collected tree-ring cores of forest hemlock (*Tsuga forrestii*) from the
18 northwestern Yunnan area of the southeastern Tibetan Plateau (SETP), and created a residual tree-ring width (TRW)
19 chronology. An analysis of the relationship between tree growth and climate revealed that precipitation during the non-growing
20 season (NGS) (from November of the previous year to February of the current year) was the most important constraining factor
21 on the radial tree growth of forest hemlock in this region. In addition, the influence of NGS precipitation on radial tree growth
22 was relatively uniform over time (1956–2005). Accordingly, we reconstructed the NGS precipitation over the period spanning
23 from A.D. 1600–2005. The reconstruction accounted for 28.5% of the actual variance during the common period 1956–2005.
24 Based on the reconstruction, NGS was extremely dry during the years A.D. 1656, ~~1670~~, 1694, 1703, 1736, 1897, 1907, 1943,
25 ~~1969~~, 1982, and 1999. In contrast, the NGS was extremely wet during the years A.D. 1627, 1638, 1654, 1832, 1834–1835, and
26 1992. Similar variations of the NGS precipitation reconstruction series and Palmer Drought Severity Index (PDSI)
27 reconstructions of early growing season from surrounding regions indicated the reliability of the present reconstruction. A
28 comparison of the reconstruction with Climate Research Unit (CRU) gridded data revealed that our reconstruction was
29 representative of the NGS precipitation variability of a large region in the SETP. Our study provided with the first historical

30 NGS precipitation reconstruction in the SETP which enriches the understanding of the long-term climate variability of this
31 region. The NGS precipitation showed slightly increasing trend during the last decade which might accelerate regional forest
32 hemlock growth.

33 **Keywords:** Tree rings; Non-growing season precipitation; Reconstruction; Southeastern Tibetan Plateau

34 **1 Introduction**

35 Unravelling the past climate often relies on proxy records. As a widely used proxy material, tree rings provide an opportunity
36 to obtain long-term climate data (Fritts, 1976; Esper et al., 2002; D'Arrigo et al., 2005; Li et al., 2011; Büntgen et al., 2011,
37 2016; Cai et al., 2014; Yang et al., 2014; Schneider et al., 2015; Wilson et al., 2016; Keyimu et al., 2021). These long-term
38 records enable us to identify the inter-annual, decadal and multi-decadal variability of historical climatic conditions. They also
39 provide a reference to better understand the nature of current climatic conditions (warming/cooling, drying/wetting) and to
40 project the future regional climate, as well as the dynamic response of earth processes (e.g., forest growth, glacier
41 retreat/advance, stream flow, drought frequency, and forest fires) to climate change.

42 Being the “third pole” of the Earth, the Tibetan Plateau (TP) (average 4000 m a.s.l.) is particularly sensitive to climate change
43 and is one of the fastest warming places in the world (Chen et al., 2020). The average decadal temperature increase at the TP
44 is 0.33°C, which is higher than the world’s average decadal temperature increase of 0.20°C (Yan and Liu, 2014). Because of
45 its geographical extent and position within the global circulation system, the TP plays a key role in regional and global
46 atmospheric circulation patterns (Griessinger et al., 2017), not only affecting the mid-latitude westerlies, but also influencing
47 the Asian monsoon circulation through its thermo-dynamical feedbacks (Duan et al., 2006; Rangwala, 2009; Wu et al., 2015).

48 There are large areas of coniferous forest distributed at high altitudes in the southeastern Tibetan Plateau (SETP). Due to
49 their age and relative lack of disturbance they are a source of proxy material (tree rings) that can be used to reveal the past
50 climatic conditions in this region (Bräuning and Mantwill, 2004; Fan et al., 2009; Fang et al., 2010; Li et al., 2011; Wang et
51 al., 2015; Li and Li., 2017; Shi et al., 2017; Huang et al., 2019; Shi et al., 2019; Keyimu et al., 2021). Many
52 dendroclimatological reconstructions of hydroclimatic variables have also been conducted in the SETP (Fan et al., 2008; Zhang
53 et al., 2015; Wernicke et al., 2015; Griessinger et al., 2017; Li et al., 2017; He et al., 2018). However, few studies have focused
54 on the reconstruction of precipitation history (He et al., 2012; Wernicke et al., 2015). The non-growing season (NGS) of
55 vegetation (from November of the previous year to February of the current year) includes the ~~non-winter~~ monsoon and pre-
56 summer monsoon seasons in the SETP, and water availability during the NGS might therefore have a constraining effect on
57 radial tree growth (Linderholm and Chen, 2005). It is important to understand the long-term precipitation variations during the
58 NGS to evaluate the current trend of precipitation variation and estimate its future patterns, and to determine the future
59 responses of the forest ecosystem under the changing precipitation trend. To our knowledge, however, there have been no

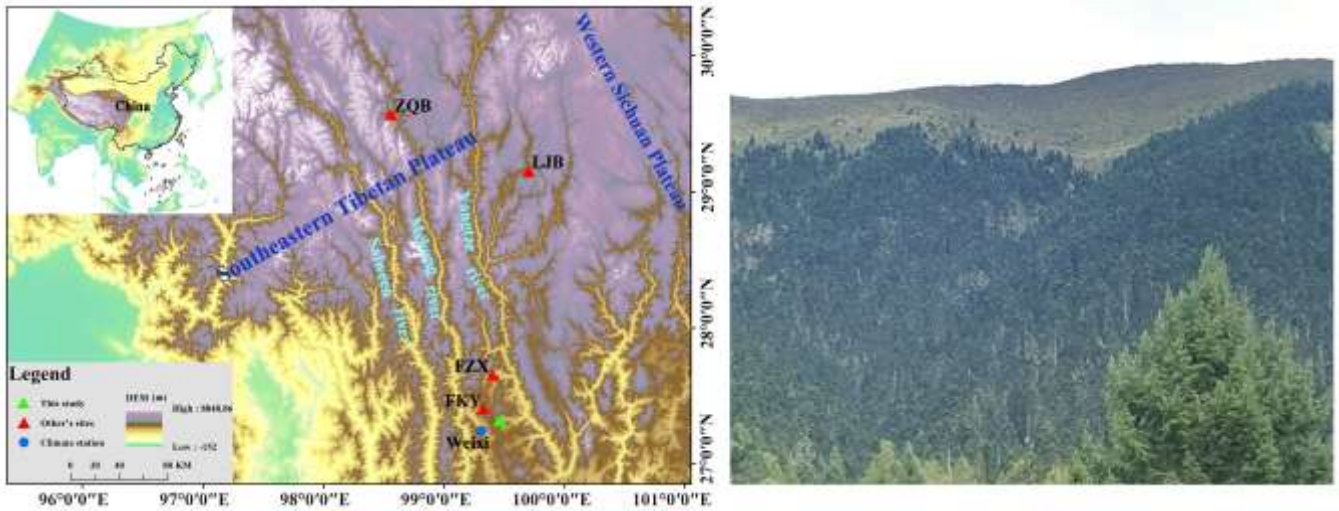
60 reports of the reconstruction of NGS precipitation in this area. This hinders our understanding of NGS variability from a long-
61 term perspective.

62 In this study, we collected tree-ring cores of forest hemlock from the Xinzhu Village of northwestern Yunnan in the SETP.
63 The main objectives of the present study were to (1) develop a new tree-ring chronology and identify the responses of forest
64 hemlock radial growth to climate in the investigation area ~~relationship between the radial growth of forest hemlock and climate,~~
65 (2) reconstruct the ~~regional precipitation history~~ historical climate ~~NGS precipitation change~~ and evaluate the recent
66 climate ~~NGS precipitation change in the long-term context,~~ and (3) validate the reliability of the reconstruction. Our results not
67 only ~~improve~~ enrich the historical ~~precipitation~~ hydro-climatic information available in the SETP, but also provide ~~the~~ with
68 basis to ~~evaluate~~ understand the current trend of regional NGS precipitation variation, ~~as well as the~~ which is relevant for
69 evaluating the future development of regional forest ecosystem ~~growth~~.

70 2 Materials and methods

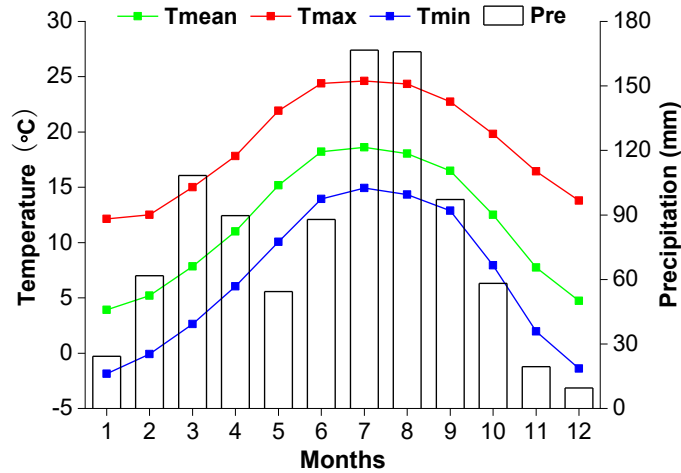
71 2.1 Study area and sampling sites

72 Tree-ring core samples were collected from Xinzhu Village in Lijiang County in northwestern Yunnan. The sample site was
73 in the Hengduan Mountains in the SETP (Fig. 1). The climate of the study area is regulated by a westerly circulation and the
74 monsoon circulations of the Indian and Pacific oceans. “Hengduan” means “transverse” in the Chinese language, which implies
75 that the mountains in this region lie in the transverse direction from south to north, and the area is a passageway for the Indian
76 monsoon to flow in and climb up to the TP and other parts of the mainland. The SETP is susceptible to monsoon flow and
77 atmospheric circulations (Bräuning and Mantwill, 2004). According to the Weixi meteorological station of the China
78 Meteorological Administration, which was the closest station to our sampling site, the mean annual precipitation was 953 mm
79 from 1955 to 2016. Most of the annual precipitation (Nearly 70%) concentrated in the monsoon season from May to October
80 in this region (Fig. 2), and thus, tree growth is usually constrained by water availability during non-growing season. The coldest
81 temperature was -2.9°C in January and the warmest temperature was 18.6°C in July. The topography of the sampling area is
82 relatively steep, and it is not in favour of the soil development, hence, thin soil layer of alpine meadow soil (Chinese soil
83 taxonomy) covers the bedrock. Forest hemlock is the dominant tree species of the sampling site, and its t ~~ree-ring cores of~~
84 ~~forest hemlock~~ were collected from trees which are healthy and relatively isolated, an optimal condition for maximizing climate
85 signals in tree rings (Li et al., 2017). ~~-at a site that had not been impacted by anthropogenic disturbances.~~ The elevation of the
86 sampling site was 2,966 m a.s.l. A total of 48 tree-ring cores were extracted from 48 trees using a 5.1 mm diameter increment
87 borer. We have used one sampling per tree method to improve the spatial representativity of radial tree growth. Sampling was
88 conducted along an axis perpendicular to the slope inclination to avoid the impact of tension wood (Keyimu et al., 2020).



89

90 **Figure 1:** Map of the study area. The green triangle is the study site. The red triangles are the sites in other studies (previous year May –
 91 current year April PDSI reconstruction site in Fang et al., 2010; current year March – May PDSI reconstruction site in Fan et al., 2008;
 92 current year April – June PDSI reconstruction site in Li et al., 2017; current year May – June PDSI reconstruction site in Zhang et al., 2015).
 93 The blue dot is the meteorological station in Weixi County. On the right is the landscape image of tree ring sampling site.
 94



95

96 **Figure 2:** The ombrothermic diagram of the climate variables in the study area

97 **2.2 Establishment of the tree-ring chronology**

98 The tree-ring samples were treated with standard dendrochronological procedures. They were first glued onto wooden holders
 99 and air-dried, and then polished to a flat surface with sand paper until the tree rings were clearly visible. The LINTAB 6.0 tree

100 ring measurement system was used to measure the tree-ring width (TRW). ~~Crossdating was conducted visually by~~ We have
101 marked the tree rings of each sample at each ten-year interval and visually checked the ~~crossdating-tree ring pattern~~
102 matching among samples, and then its quality was confirmed the crossdating quality using the COFFECHA program (Holmes,
103 1983). Thirty-eight of the tree-ring cores were adopted for a further analysis after excluding the bad quality samples and the
104 un-crossdated samples. The tree-ring series was detrended with a negative exponential model to remove the age dependency
105 of tree growth (Cook et al., 1995). We have used the residual chronology since it removes the auto-correlation in tree ring
106 growth and captures high frequent climate signal. The “dplR” software toolkit (Bunn, 2018) within the R software environment
107 (R Core Team 2020) was used for detrending and chronology establishment. The reliable period of the chronology was
108 determined based on the criterion of expressed population signal (EPS) > 0.85 (Wigley, 1984).

109 **2.3 Climate data**

110 Temperature and precipitation records were obtained from the Weixi meteorological station (27.17° N, 99.28° E, 2326 m a.s.l.)
111 operated by the China Meteorological Administration. Data was available for the period of 1955–2005. Climate data (including
112 the maximum, minimum and average temperatures, and precipitation) were provided by the China Meteorological Data
113 Sharing Service Platform. A self-calibrated Palmer Drought Severity Index (scPDSI) was downloaded from the 3.26e gridded
114 dataset of the Climate Research Unit (CRU) via the Royal Netherlands Meteorological Institute (KNMI) climate explorer (data
115 accessed on 23rd December, 2020, data re-accessed for the updated version (CRU scPDSI 4.05 early) of PDSI data on 20th of
116 April, 2021) using the coordinates of the tree ring sampling site. The range of CRU grid box is 27.0 – 27.5° N, 99.0 – 99.5° E.

117 **2.4 Tree growth and climate relationship analysis**

118 We analysed the relationship between climate and tree growth using Dendroclim 2002 software (Biondi and Waikul, 2004).
119 Pearson correlation values and response function values were calculated for the relationships between TRW indices and climate
120 variables for the period of 1955–2005. Due to the carry over effect of the climatic conditions of the previous-year on the current
121 year tree growth (Fritts, 1976), the tree growth – climate relationship analysis spanned a 16-month period from June of the
122 previous year to September of the current year. We also used the seasonalised climate variables because it made more eco-
123 physiological sense for growth than single months. To observe the temporal stability of the climate influence on radial tree
124 growth, we conducted a moving correlation analysis at a moving interval of 32 years. All the correlation results were considered
125 significant at the 95% confidence level.

126 **2.5 Statistics of chronology and Climate reconstruction**

127 We have used the expressed population signal (EPS) to determine the reliable period of the chronology; mean inter-series
128 correlation (Rbar), signal-to-noise ratio (SNR) and variance of first eigenvector (VFE) to evaluate the common signal among
129 measurement series; standard deviation (SD) and mean sensitivity (MS) to show the degree of inter-annual variability of the

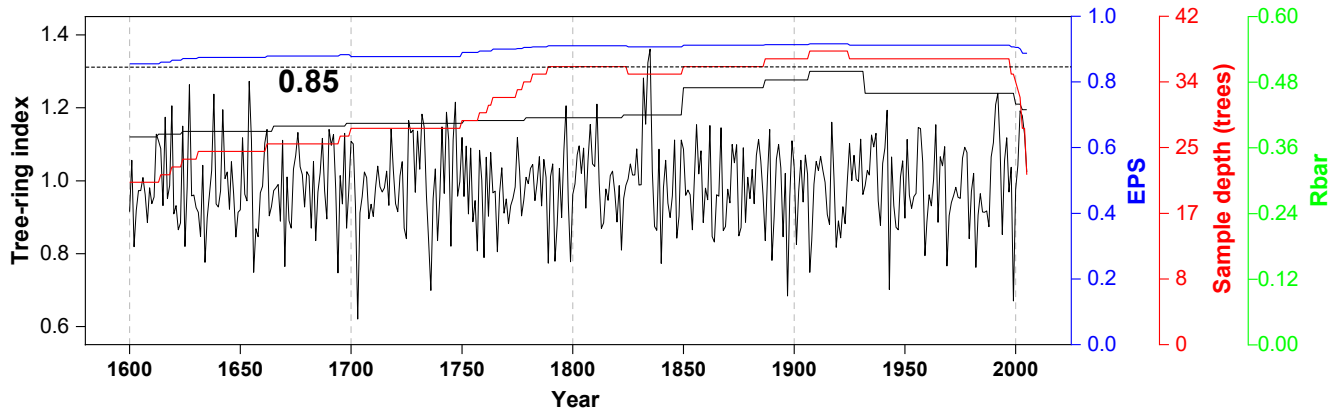
130 chronology. According to the analysis of the relationship between the TRW indices and constraining climatic factors, we
 131 developed a linear regression model (Cook and Kairiukstis, 1990) for the climate reconstruction. As in many other tree ring
 132 based climate reconstructions, we tested the goodness-of-fit of the model using the leave-one-out cross-validation method
 133 (Michaelsen, 1987). We used the Pearson's correlation coefficient (r), explained variance (R^2), adjusted explained variance
 134 (R_{adj}^2), reduction of error (RE), sign test (ST), coefficient of efficiency (CE), and product mean test (Pmt) to evaluate the
 135 fidelity of the reconstruction model (Fritts et al., 1990).

136 3. Results

137 3.1 Characteristics of the TRW chronology

138 Residual TRW chronology of forest hemlock from the investigation area was established (Fig. 3). The descriptive statistics of
 139 the chronology were presented in Table 1. According to the criteria of $EPS > 0.85$, the most reliable length of the TRW
 140 chronology was 406 years (A.D. 1600–2005). The mean correlation among tree-ring series (R_{bar}) was 0.48, and the variance
 141 in the first eigenvector (VFE) was 27 %, which implied a relatively strong common signal among individual trees constituting
 142 the chronology. The relatively low inter-annual variability of the chronology was expressed by the small mean sensitivity value
 143 (0.23). The EPS and SNR values (average EPS and SNR were 0.89 and 6.87 for the total length chronology, respectively)
 144 further implied the existence of the common signal among each individual measurement series. In general, all the statistical
 145 parameters indicated the potential climate signal imprinted in our TRW chronology.

146



147

148 **Figure 3:** Plot of tree-ring residual chronology, the running inter-correlations among cores (R_{bar} , the green line), expressed population
 149 signal (EPS, the blue line) and the sample size (the red line). The R_{bar} and EPS were calculated using a 30-year window, with a 15-year lag.
 150 The horizontal dashed line denotes the EPS threshold level (0.85).

151

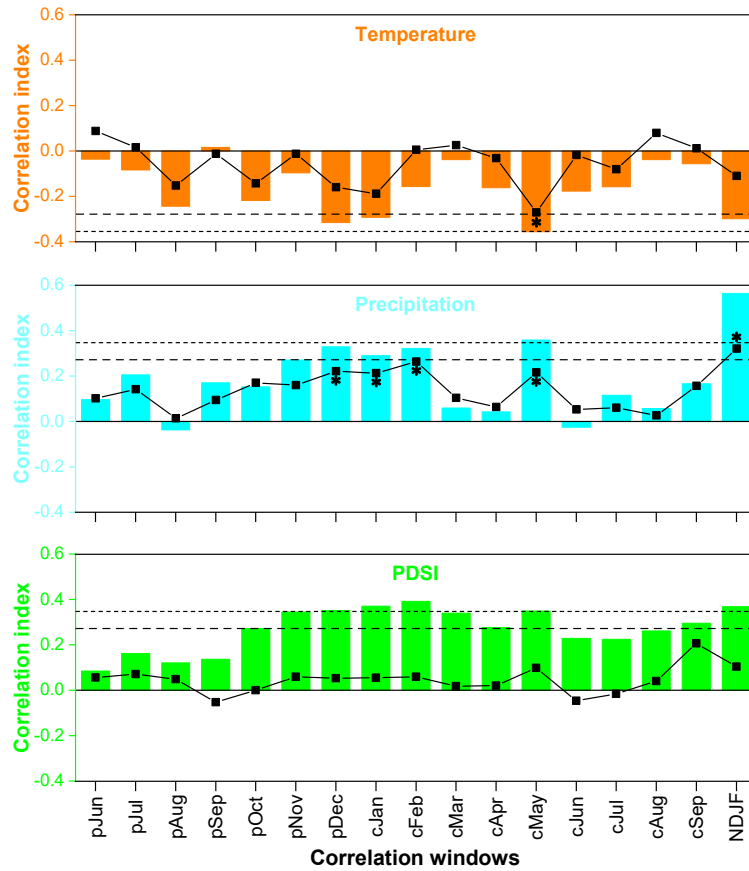
152 Table 1. Site information, chronology statistics and results of a common interval span analysis of residual tree-ring width
153 (TRW) chronology from the Xinzhu Village, northwestern Yunnan in China

Type	Location	Elevation (m)	Time length	Number of cores	SD	MS	Rbar	SNR	EPS	VFE
Tree ring	99.43°E, 27.25°N	2966	1600–2005	38	0.22	0.23	0.48	6.87	0.89	0.27

154 Note: SD: standard deviation, MS: mean sensitivity, Rbar: mean inter-series correlation, SNR: signal-to-noise ratio, EPS: Expressed
155 Population Signal, VFE: Variance in first eigenvector.

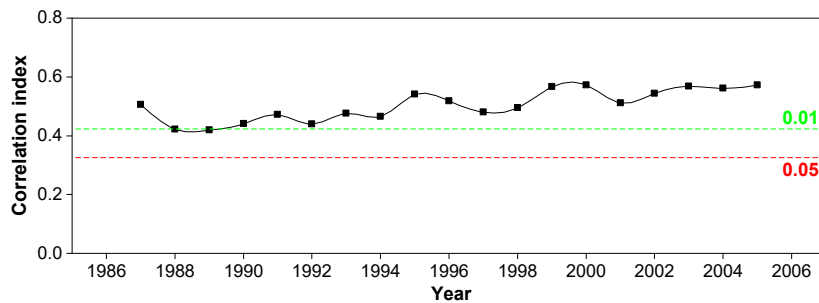
156 **3.2 Tree growth and climate relationship analysis**

157 According to the results of the tree growth and climate relationship analyses (Fig. 4), the precipitation during the NGS was the
158 most important constraining factor ($R = 0.56$, $p < 0.001$) on the radial growth of forest hemlock in the study area. The results
159 of a response function analysis further confirmed the strong correlation between NGS precipitation and forest hemlock radial
160 growth. The results of a moving correlation analyses between TRW chronology and instrumental NGS precipitation record
161 (Fig. 5) were positively significant (at 99%) during the investigated period (1956-2005), indicating that the NGS precipitation
162 influence was stationary over time.



163

164 **Figure 4:** Correlations between tree-ring indices and temperature, precipitation, and scPDSI in the correlation windows from
 165 previous year June to current year September, as well as in NDJF (non-growing season, NGS) for the common period from
 166 1956 to 2005. The horizontal dashed and dotted lines indicate the threshold of the correlations at the 95% and 99% significance
 167 levels. Black line with squares denotes the results of response function analysis between tree-ring indices and climate variables.
 168 The asterisks next to the squares denote the significant effects ($p < 0.05$) of response function analyses.

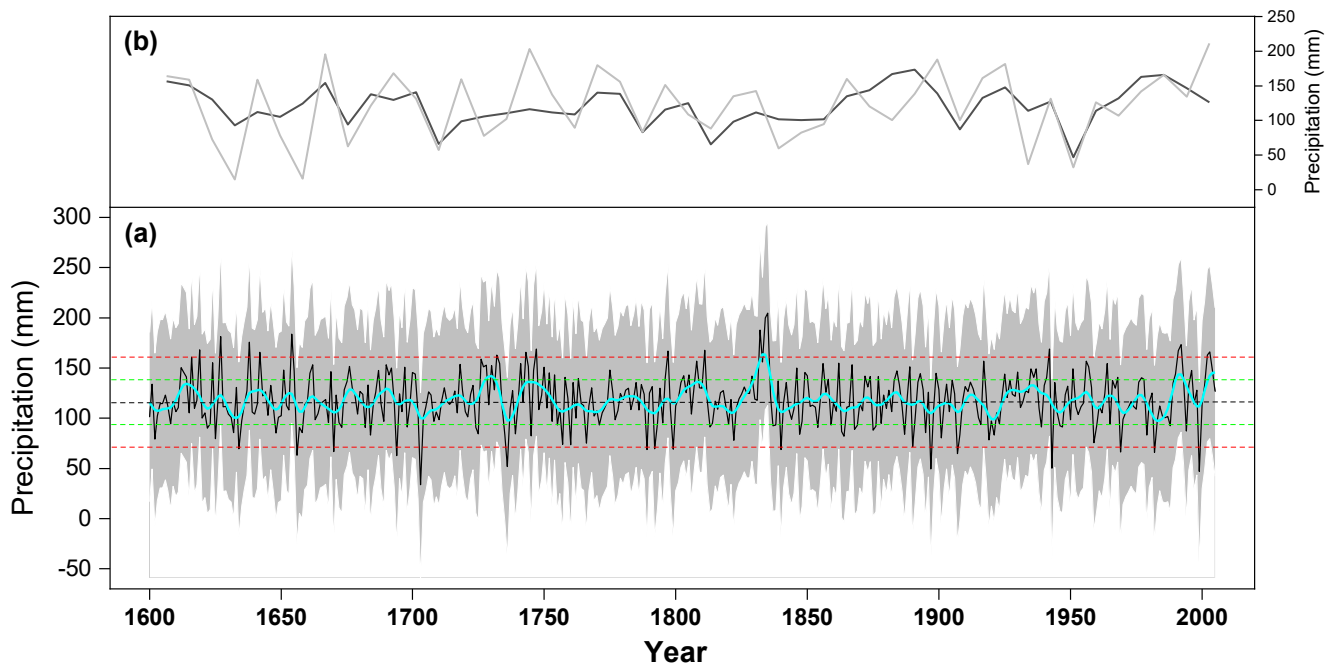


169

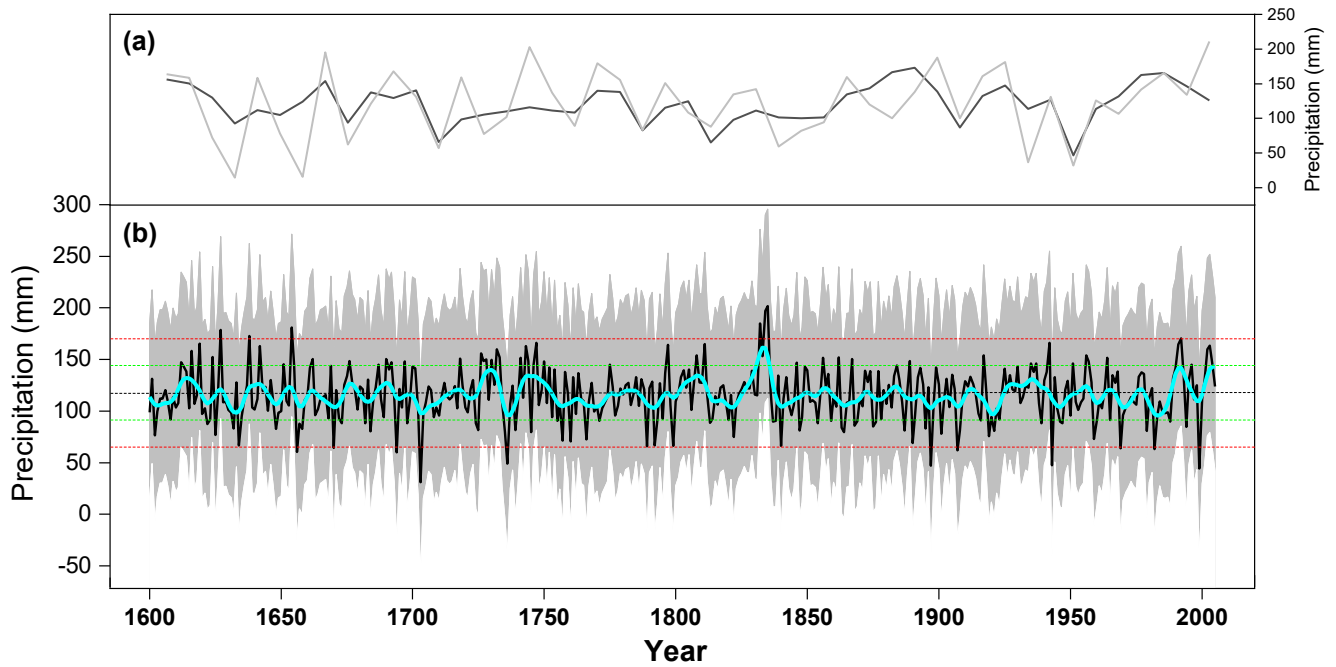
170 **Figure 5:** The moving correlation result between tree-ring width (TRW) chronology and non-growing season (NGS) precipitation during
171 the period of 1956–2005. The horizontal red and green dashed lines denote the significance levels of 0.05 and 0.01, respectively.

172 3.3 Non-growing season precipitation reconstruction

173 According to the relationship between the TRW chronology and NGS precipitation, we developed a linear regression model
174 ($y = 229.94x - 109.45$ mm) and reconstructed the historical NGS precipitation series, which extended back to A.D. 1600 (Fig.
175 [6a6b](#)). In the model, y is the NGS precipitation, and x is the TRW index. The reconstruction accounted for 28.5% of the
176 instrumental NGS precipitation variability during the common time span (1956–2005). Figure [6b-6a](#) shows the similarities
177 between the instrumental and reconstructed NGS precipitation series. We used a leave-one-out cross-verification method to
178 evaluate the legitimacy of the reconstruction model (Table 2). The positive RE and CE values (0.18 and 0.15, respectively)
179 were indicative of legitimacy of the reconstruction. The significant value (at 95%) of sign test implied that the model predicted
180 values were generally in line with the variation trend of instrumental values. In addition, the significant values of F test (at
181 99%) and PM test (at 95%) further confirmed the validity of the reconstruction. Overall, the statistics indicated that the
182 reconstruction model possessed good predictive skills.



183



184

185 **Figure 6:** Non-growing season (NGS) precipitation reconstruction from A.D. 1600 to 2005. (a) The black line is the
 186 reconstruction series, the thick cyan line is the 11- year loess smoothed series. The horizontal black dashed line is the mean of
 187 NGS precipitation value during from A.D. 1600–2005. The horizontal green and red dashed lines are the one time and two
 188 times the of standard deviations of NGS precipitation, which demonstrated the boundaries of dry and extremely dry (below
 189 mean), and wet and extreme wet (above mean) years. The grey shading indicated the 95% confidence interval of the
 190 reconstruction; (b) Instrumental (black) and reconstructed (grey) NGS precipitation during their common period of 1956–2005.
 191

192

Table 2. Leave-one-out verification statistics for the non-growing season (NGS) precipitation reconstruction

	R	R^2	R_{adj}^2	F	Sign-test	Pmt	RE	CE
Calibration	0.561	0.315	0.285	–	–	–	–	–
Verification	0.524	0.274	0.235	18.6**	36+/13–*	7.89*	0.18	0.15

193 Note: R correlation coefficient, R^2 explained variance, R_{adj}^2 is the adjusted explained variance, F F -test, Sign-test sign of paired observed
 194 and estimated departures from their mean on the basis of the number of agreements/disagreements, Pmt product mean test, RE reduction of
 195 error, CE coefficient of efficiency. * $p < 0.05$, ** $p < 0.01$

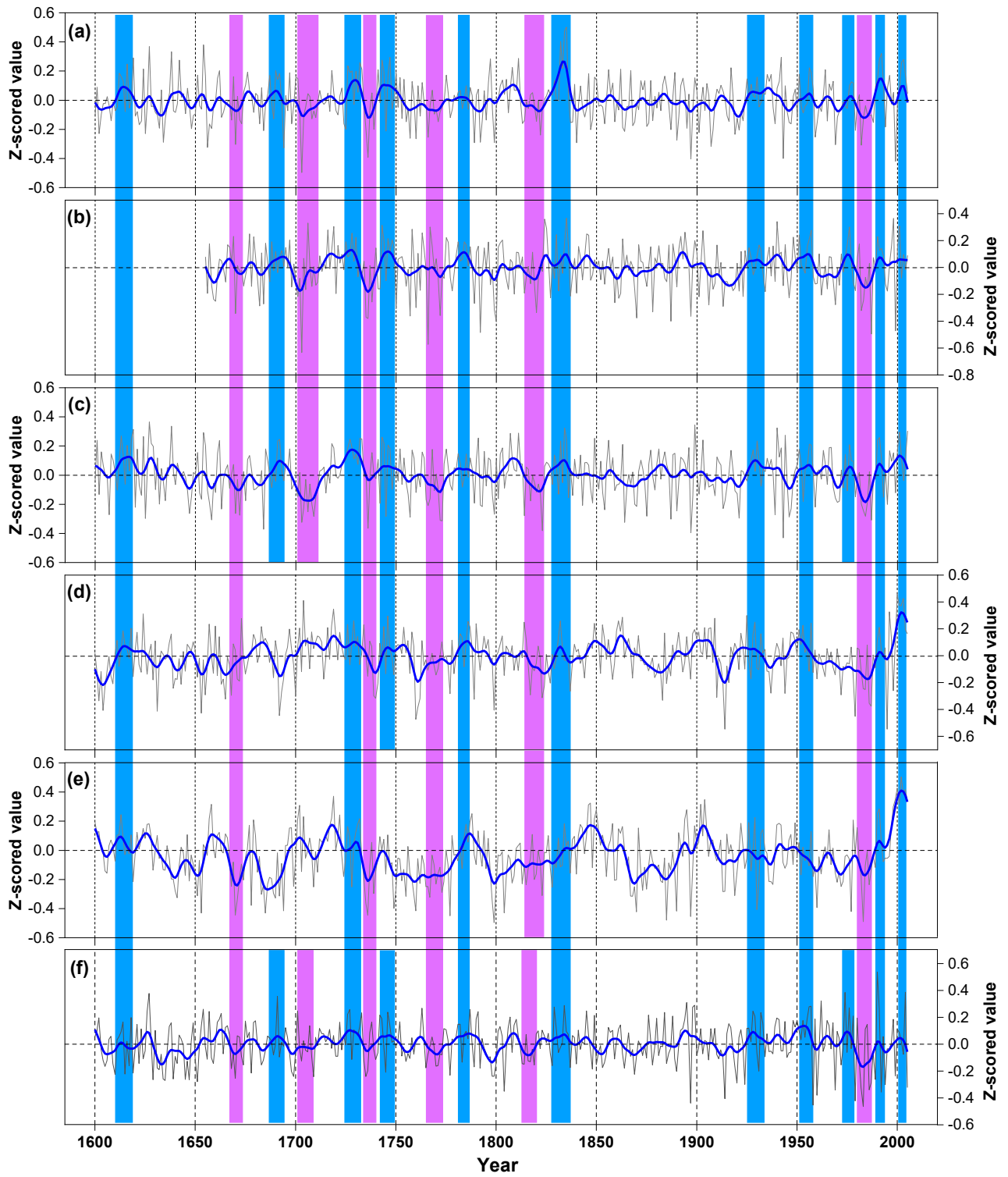
196 **3.4 Characteristics of the NGS precipitation reconstruction**

197 Figure ~~6a-6b~~ shows the reconstructed NGS precipitation over the past 406 years (A.D. 1600–2005). The mean of the
 198 reconstructed NGS precipitation series was ~~117.87~~ mm, and the standard deviation (SD) was ~~25.64~~ mm. We pre-defined the
 199 years that had NGS precipitation ~~below 92.23~~ above 144 mm (mean₊–SD) as ~~wet~~ dry NGS years, and ~~below 66.59~~ above 170
 200 mm (mean₊–2SD) as extremely ~~wet~~ dry years (Table 3), whereas we defined years that had precipitation ~~above below 143.51~~ 192
 201 mm (mean_–+SD) as ~~dry~~ wet NGS years, and ~~above below 169.15~~ 66 mm (mean_–+2SD) as extremely ~~dry~~ wet NGS years (Table
 202 ~~3~~). ~~Accordingly, the NGS was extremely dry during the years A.D. 1656, 1670, 1694, 1703, 1736, 1897, 1907, 1943, 1969,~~
 203 ~~1982, and 1999. In contrast, the NGS was extremely wet during the years A.D. 1627, 1638, 1654, 1832, 1834–1835, and 1992.~~
 204 The dry/wet periods and some of the extreme dry/wet NGS periods in the present reconstruction were synchronised with
 205 dry/wet periods and extreme dry/wet periods in previously reported PDSI reconstruction from the surrounding region (Fig. 7,
 206 Table S2, Table S3), though some dissimilarities were also existed. As shown in Fig. 8, the instrumental (**a, c**) and reconstructed
 207 (**b, d**) NGS precipitation series could represent the climatic conditions over a similar area in the SETP.

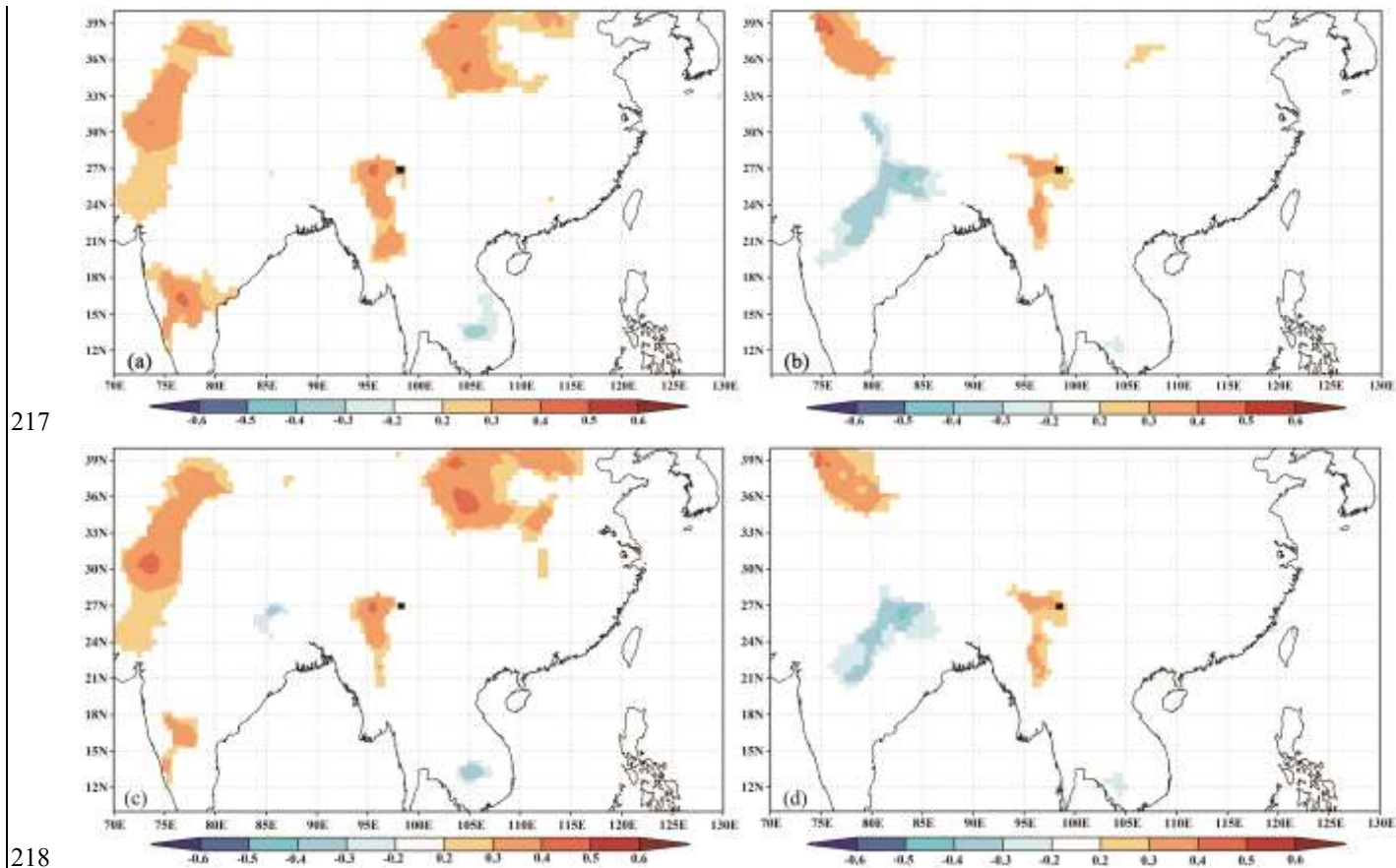
208

Table 3 Extreme wet and dry NGS years

<u>Year</u>	<u>Dry (mm)</u>	<u>Year</u>	<u>Wet (mm)</u>
<u>1656</u>	<u>63</u>	<u>1627</u>	<u>181</u>
<u>1694</u>	<u>62</u>	<u>1638</u>	<u>175</u>
<u>1703</u>	<u>33</u>	<u>1654</u>	<u>183</u>
<u>1736</u>	<u>51</u>	<u>1832</u>	<u>187</u>
<u>1897</u>	<u>49</u>	<u>1834</u>	<u>199</u>
<u>1907</u>	<u>64</u>	<u>1835</u>	<u>204</u>
<u>1943</u>	<u>50</u>	<u>1992</u>	<u>173</u>
<u>1982</u>	<u>65</u>		
<u>1999</u>	<u>47</u>		



210 **Figure 7:** Comparisons of the hydroclimatic reconstructions in different studies. (a) The non-growing season (NGS)
211 precipitation reconstruction in the present study. (b) The current year March – May average Palmer Drought Severity Index
212 (PDSI) reconstruction in Fan et al. (2008). (c) The reconstruction of average PDSI from May of the previous year to April of
213 the current year in Fang et al. (2010). (d) The current year May-June average PDSI reconstruction in Zhang et al. (2015). (e)
214 The current year April-June average PDSI reconstruction in Li et al. (2017). (f) drought series extracted from Asian Monsoon
215 Atlas from the nearest point (Cook et al. 2010). The blue and purple bars show the common wet and dry periods of the different
216 reconstructions, respectively.



219 **Figure 8:** Spatial correlations ~~between the of~~ actual (a: raw data; c: first-differenced data) and reconstructed (b: raw data; d:
220 first-differenced data) non-growing season (NGS) precipitation ~~and with~~ a gridded dataset of the NGS precipitation (average
221 from November of the previous year to February of the current year) during their overlapping periods (1956–2005). The black
222 square indicates the location of the study site.

223 4. Discussion

224 4.1 Tree growth and climate relationship

225 The results of the tree growth and climate relationship analyses suggested that the forest hemlock radial growth in the
226 northwestern Yunnan region of the SETP was strongly constrained by hydroclimatic factors. According to the Pearson
227 correlation analysis, the influence of precipitation during the NGS on radial tree growth was greater than that of any other
228 investigated climate variables and any correlation window. The response function analysis further confirmed the strong impact
229 of NGS precipitation. In addition, the results of 32-year interval of moving correlation analysis (Fig. 5) suggested the
230 temporally consistent influence of NGS precipitation on forest hemlock radial growth in this region. The importance of NGS
231 precipitation on the radial tree growth could be attributed to the fact that precipitation during the NGS compensated for the
232 soil moisture, which was crucially important for supporting tree growth in the following season (Linderholm and Chen, 2005;
233 Treydte et al. 2006; Wu et al., 2019; Li et al., 2021). This is because tree growth is often water stressed in the early stages of
234 its growth in each year on the SETP when the monsoon precipitation does not arrive (Bräuning and Mantwill, 2004; Zhang et
235 al., 2015), and the earlywood of tree rings mainly use spring melt water (Zhu et al., 2021). The eco-physiological importance
236 of NGS precipitation on tree growth and tree water usage was also revealed by isotope ratios method-based investigations.
237 Brinkmann et al's (2018) study showed that nearly 40% of the uptaken water by *Fagus sylvatica* and *Picea abies* trees in a
238 temperate forest of middle Europe are sourced from NGS precipitation. Tree-ring oxygen isotope ratios ($\delta^{18}\text{O}$) are
239 demonstrated to contain NGS precipitation signals in the Himalayan region (Huang et al., 2019; Zhu et al., 2021). Huang et
240 al's (2019) study revealed that NGS precipitation (snowfall) increased the snow-depth and the later snowmelt compensated
241 soil moisture in the spring and early summer, which was a crucially important water source for the Juniper growth in the
242 southwestern Tibetan Plateau. Zhu et al's (2021) investigation in the western Himalaya revealed that formation of earlywood
243 in tree rings of *Pinus wallachina* depended on the snowmelt originated from NGS precipitation. The weak influence of
244 precipitation on regional forest hemlock growth during March and April and strong influence during May was connected with
245 the saddle-shaped monthly rainfall pattern of this area (Fig. 2). The highest correlation between precipitation and TRW
246 chronology was observed in May of the current year. This is because the ~~active~~ xylogenous activity to form earlywood
247 coincided with the low precipitation in this month (Fig. 2). In addition, the melt water was probably used up (tree uptake +
248 evaporation) during the early spring. Therefore, water stressed was increased during the late spring (May). The correlations
249 between precipitation and the TRW chronology were not significant during the growing season (June-September) because an
250 adequate water supply was available in the summer monsoon season.

251 Precipitation during the NGS over the SETP falls as snow. According to Sommerfeld et al. (1993) and Stadler et al. (1996),
252 the development of a snowpack insulates the underlying soil from freezing temperatures, which creates unfrozen soil
253 conditions and most of the soil processes that are active during warmer conditions also persist under snow cover, albeit at a
254 reduced rate (Edwards, 2007). Unfrozen soil can reduce the cold and frost damage to the shallow root systems of conifer trees

255 in this region (Schenk and Jackson, 2002). A reduction in the cold damage to roots decreases the energy required to form new
256 roots in the following growth year (Pederson et al., 2004), with the saved energy potentially used to initiate xylogenesis and
257 form earlywood cells. Evergreen tree species are known to carry out year-round photosynthetic activity (Oquist and Huner,
258 2003; Prats and Brodersen, 2020), albeit at a slower rate during the NGS, and therefore, the higher moisture availability
259 contributes to the carbohydrate and energy accumulation process of forest hemlock in the investigation area.

260 In contrast, the radial tree growth was negatively correlated to temperature in most correlation windows (Fig. 4). This can
261 be explained by the fact that higher temperature enhances evapotranspiration, and thus decreases water availability, which
262 eventually constrains tree growth. The negative impact of NGS temperature on radial tree growth was obvious because the
263 strengthened evaporation due to higher temperatures might reduce the moisture compensation to the soil layer and cause water
264 stress during the early stage of the following growth season.

265 4.2 Validity of the reconstructed precipitation series

266 We have tried to validate the fidelity of the newly reconstructed series from different aspects. Although we used the residual
267 TRW chronology in the present study, which removes autocorrelation (Cook and Kairiukstis, 1990) to capture the high
268 frequency climate signals as in Fan et al. (2008) and Chen et al. (2016), the variability of dry and wet NGS at different scales
269 was still retained in ~~our~~the reconstructed series. The reconstructed series in the present study demonstrated the variation in
270 dry and wet NGS years (Fig. ~~6a~~6b). As in many other proxy based historical climate reconstruction studies, we compared our
271 NGS precipitation series with other hydroclimatic reconstructions from the surrounding areas to investigate the reliability of
272 our reconstruction. However, there was no reported historical NGS precipitation record in the SETP, and we had to compare
273 the present reconstruction series with available hydro-climatic reconstructions, e.g., PDSI. There are only countable numbers
274 of ~~hydroclimatic~~ (PDSI) reconstructions in the nearby region, ~~and not any ease of precipitation reconstruction.~~ Hence, we
275 could only compare the present NGS precipitation reconstruction with existing PDSI reconstructions (Fig. 7). ~~The compared~~
276 PDSI reconstructions which are of spring or early summer, ~~because drought, Dry/wet~~ climate during these seasons are usually
277 associated with the winter precipitation, hence, it makes certain sense to carry out the ~~comparative analysis~~ison. The correlation
278 coefficients between our NGS precipitation reconstruction and the PDSI reconstructions of Fan et al. (2008), Fang et al. (2010),
279 Zhang et al. (2015) and Li et al. (2017) were 0.51 (n = 702), 0.35 (n = 1062), 0.25 (n = 1062) and 0.22 (n = 1016) ($p < 0.001$).
280 We have extracted the drought series of Asian Monsoon Atlas (Cook et al.2010) from the nearest point to our investigation
281 site and compared it with the NGS precipitation reconstruction in present study ($R = 0.35$, n = 1062, $p < 0.001$). As can be
282 observed from Fig. 7, there were dry and wet periods in compared reconstruction series which were consistent with the NGS
283 precipitation variabilities. These similarities indicated the reliability of our NGS precipitation reconstruction to some extent.
284 The correlation coefficients for the present reconstruction with those of Fan et al. (2008) and Fang et al. (2010) were greater
285 than those with Li et al. (2017) and Zhang et al. (2015). These differences were probably due to the different distances among
286 the study sites. Although, the major dry and wet periods were similar in the hydroclimatic reconstructions referenced above,

287 there were still certain discrepancies in duration and the strength of the dry/wet climatic conditions. This is probably because
288 of the differences in the types of hydroclimatic variables (precipitation, PDSI), specific seasons reconstructed (annual,
289 seasonal), tree species (species with different drought tolerances), chronology recording methods (standard chronology,
290 residual chronology), length of calibration period, sample replication and the geomorphic differences of the tree ring sampling
291 sites (altitude, slope) (Table S1).

292 In addition, we uploaded both of the instrumental and reconstructed NGS precipitation data for the same period of 1956–
293 2005 on the KNMI website and conducted a ~~spatial correlation analyses~~spatial correlation analysis with the CRU gridded
294 climate dataset. The similar patterns of spatial correlation between the instrumental and reconstructed data and their first
295 differenced dataset (Fig. 8) indicated that the present reconstruction was reliable and could represent the NGS precipitation
296 over a large area in the SETP. Besides, the occurrence of some historical great drought events in the Asian monsoon area
297 (Cook et al., 2010, Kang et al., 2013), i.e., the 1756–1768 (strange parallels drought), 1790, 1792–1796 (east India drought)
298 and 1920s (China mega-drought), matched the dry NGS periods in our reconstruction, which also further confirmed the
299 reliability of our reconstruction.

300 5. Conclusion

301 In this study, we investigated 406 years of residual TRW chronology of forest hemlock in the SETP, China. The climate and
302 tree growth relationship analyses showed that the TRW chronology was mostly negatively correlated with the thermal variable
303 (temperature), whereas it was positively correlated with hydroclimatic variables (precipitation) and PDSI, indicating that
304 hydroclimatic conditions determined the radial growth of forest hemlock in this region. Accordingly, we derived a linear model
305 of the relationship between climate and tree growth, which accounted for 28.5% of the actual NGS precipitation variance
306 (1956–2005), and we used the model to reconstruct the historical (A.D. 1600–2005) NGS precipitation. The reconstructed
307 series showed that the NGS was extremely dry during the years A.D. 1656, ~~1670~~, 1694, 1703, 1736, 1897, 1907, 1943, ~~1969~~,
308 1982 and 1999. In contrast, the NGS was extremely wet during the years A.D. 1627, 1638, 1654, 1832, 1834–1835 and 1992.
309 A comparison between the NGS precipitation reconstruction in this study and PDSI reconstructions from nearby regions
310 revealed a coherency in the timing of dry and wet episodes, suggesting the reliability of our reconstruction. Our results showed
311 that the NGS precipitation showed demonstrated slightly increasing trend since 1980s which is in favour of the future forest
312 ecosystem development. In the future, more efforts should be made to collect wide-area of tree-ring data and develop more
313 proxy chronologies that will enable us to reveal historical precipitation variability at the longer and wider scale in the SETP.

314 **Data availability.** The climate reconstruction series in this study can be obtained from Zongshan Li after the paper publication.

315 **Author contributions.** ZSL and MK conceived the study; ZSL, ZXF, XCW collected the tree-ring data; MK, ZSL, ZXF, KYF,
316 XCW elaborated the methodology; MK, ZSL, WLC analysed the data; MK, ZSL led the writing of the manuscript; ZSL and
317 ZXF revised the manuscript; BJB and GHL validated the final manuscript.

318 **Competing interests.** The authors declare that they have no conflict of interest.

319 **Acknowledgement.** This work was funded by the National Key Research Development Program of China (2016YFC0502105),
320 the second Tibetan Plateau Scientific Expedition and Research (STEP) Program (2019QZKK0502). We are grateful to the
321 editor and anonymous reviewers for their valuable comments and suggestions to improve this article.

322 **References**

323 Biondi, F. and Waikul, K.: DENDROCLIM2002: a C++ program for statistical calibration of climate signals in tree ring
324 chronologies, *Comput. Geosci.*, 30(3), 303-311, <https://doi.org/10.1016/j.cageo.2003.11.004>, 2004

325 Bräuning, A. and Mantwill, B.: Summer temperature and summer monsoon history on the Tibetan Plateau during the last 400
326 years recorded by tree rings, *Geophys. Res. Lett.*, 31, L24205, <https://doi.org/10.1029/2004GL020793>, 2004

327 Bunn, A. G. and Korpela, M.: An introduction to dplR. The Comprehensive R Archive Network,
328 <https://cran.biodisk.org/web/packages/dplR/vignettes/intro-dplR.pdf>, 2018

329 Büntgen, U., Myglan, V. S., Ljungqvist, F. C., McCormick, M., Di Cosmo N., Sigl, M., Jungclaus, J., Wagner, S., Krusic, P.
330 J., Esper, J., Kaplan, J. O., de Vaan MAC., Luterbacher, J., Wacker, L., Tegel, W. and Kirilyanov, A. V.: Cooling and societal
331 change during the Late Antique Little Ice Age from 536 to around 660 AD, *Nat. Geosci.*, 9, 231–236,
332 <https://doi.org/10.1038/ngeo2652>, 2016

333 Büntgen, U., Tegel, W., Nicolussi, K., McCormick, M., Frank, D., Trouet, V., Kaplan, J. O., Herzig, F., Heussner, K. U.,
334 Wanner, H., Luterbacher, J. and Esper, J.: 2500 years of European climate variability and human susceptibility, *Science*, 331,
335 578–582, <https://doi.org/10.1126/science.1197175>, 2011

336 Cai, Q. F, Liu, Y., Lei, Y., Bao, G. and Sun, B.: Reconstruction of the march-august PDSI since 1703 AD based on tree rings
337 of Chinese pine (*Pinus tabulaeformis* Carr.) in the Lingkong Mountain, southeast Chinese loess Plateau, *Clim. Past.*, 10, 509–
338 521, <https://doi.org/10.5194/cp-10-509-2014>, 2014

339 Chen, F., Yuan, Y. J, Zhang, T. W, Shang, H.: Precipitation reconstruction for the northwestern Chinese Altay since 1760
340 indicates the drought signals of the northern part of inner Asia, *Int. J. Biometeorol.*, 60(3), 455-463.
341 <https://doi.org/10.1007/s00484-015-1043-5>, 2016

342 Cook, E. R. and Kairiukstis, A.: *Methods of Dendrochronology: Applications in the Environmental Sciences*, Kluwer
343 Academic Press, Dordrecht, 1990

344 Cook, E. R., Anchukaitis, K. J., Buckley, B. M., D'Arrigo, R. D., Jacoby, G. C. and Wright, W. E.: Asian monsoon failure and
345 megadrought during the last millennium, *Science*, 328(5977), 486-489, <https://doi.org/10.1126/science.1185188>, 2010

346 Cook, E. R., Briffa, K. R., Meko, D. M., Graybill, D. A. and Funkhouser, G.: The 'segment length curse' in long tree-ring
347 chronology development for palaeoclimatic studies, *Holocene*, 5(2), 229-237. <https://doi.org/10.1177/095968369500500211>,
348 1995

349 D'Arrigo, R. D., Mashig, E., Frank, D. C., Wilson, R. J. S. and Jacoby, G. C.: Temperature variability over the past millennium
350 inferred from Northwestern Alaska tree rings, *Clim. Dynam.*, 24, 227-236. <https://doi.org/10.1007/s00382-004-0502-1>, 2005

351 Duan, K., Yao, T. and Thompson, L.: Response of monsoon precipitation in the Himalayas to global warming, *J. Geophys.*
352 *Res.*, 111, D19110. <https://doi.org/10.1029/2006JD007084>, 2006

353 Edwards, A. C., Scalenghe, R., Freppaz, M.: Changes in the seasonal snow cover of alpine regions and its effect on soil
354 processes: a review. *Quat. Int.*, 162-163, 172-181. <https://doi.org/10.1016/j.quaint.2006.10.027>, 2007

355 Esper, J.: 1300 years of climatic history for Western Central Asia inferred from tree rings, *Holocene*, 12(3), 267-277.
356 <https://org.doi.10.1191/0959683602hl543rp>, 2002

357 Fan, Z. X., Bräuning, A. and Cao, K. F.: Tree-ring based drought reconstruction in the central Hengduan Mountains region
358 (China) since AD 1655, *Int. J. Climatol.*, 28, 1879–1887, <https://doi.org/10.1002/joc.1689>, 2008

359 Fan, Z. X., Bräuning, A., Yang, B. and Cao, K. F.: Tree ring density-based summer temperature reconstruction for the central
360 Hengduan Mountains in southern China, *Glob. Planet. Change*, 65 (1-2), 1-11. <https://doi.org/10.1016/j.gloplacha.2008.10.001>,
361 2009

362 Fang, K. Y, Gou, X. H, Chen, F., Li, J. B., D'Arrigo, R., Cook, E. D, Yang, T. and Davi, N.: Reconstructed droughts for the
363 southeastern Tibetan Plateau over the past 568 years and its linkages to the Pacific and Atlantic Ocean climate variability,
364 *Clim. Dyn.*, 35(4), 577–585. <https://doi.org/10.1007/s00382-009-0636-2>, 2010

365 Fritts, H. C., Guiot, J. and Gordon, G. A.: Verification. In: Cook E and Kairiukstis LA, eds., *Methods of Dendrochronology:*
366 *Applications in the Environmental Sciences*. Dordrecht, Kluwer Academic Publishers, 178-184, 1990

367 Fritts, H. C.: *Tree rings and climate*. Academic Press, London, 1976

368 Griessinger, J., Bräuning, A., Helle, G., Hochreuther, P. and Schleser, G.: Late Holocene relative humidity history on the
369 southeastern Tibetan plateau inferred from a tree ring $\delta^{18}\text{O}$ record: recent decrease and conditions during the last 1500 years,
370 *Quat. Int.*, 430, 52–59, <http://dx.doi.org/10.1016/j.quaint.2016.02.011>, 2017

371 He, H. M., Bräuning, A., Griessinger, J., Hochreuther, P. and Wernicke, J.: May–June drought reconstruction over the past
372 821 years on the southcentral Tibetan Plateau derived from tree-ring width series, *Dendrochronologia*, 47, 48–57,
373 <https://doi.org/10.1016/j.dendro.2017.12.006>, 2018

374 He, H. M., Yang, B., Bräuning, A., Wang, J. L. and Wang, Z. Y.: Tree-ring derived millennial precipitation record for the
375 south-central Tibetan plateau and its possible driving mechanism, *Holocene*, 23 (1), 36-45,
376 <https://doi.org/10.1177/0959683612450198>, 2012

377 Holmes, R. L.: Computer-assisted quality control in tree-ring dating and measurement, *Tree-ring Bulletin*, 43, 69-75, 1983

378 Huang, R., Zhu, H. F., Liang, E. Y., Liu, B., Shi, J. F., Zhang, R. B., Yuan, Y. J., Griessinger, J.: A tree ring-based winter
379 temperature reconstruction for the southeastern Tibetan Plateau since 1340 CE, *Clim. Dyn.*, 53, 3221-3233.
380 <https://doi.org/10.1007/s00382-019-04695-3>, 2019

381 Kang, S. Y, Bao, Y., Qin, C., Wang, J. L, Feng, S., Liu, J. J.: Extreme drought events in the years 1877–1878, and 1928, in
382 the southeast Qilian mountains and the air–sea coupling system. *Quat. Int.*, 283(427), 85-92.
383 <https://doi.org/10.1016/j.quaint.2012.03.011>, 2013

384 Keyimu, M., Li, Z. S., Liu, G. H., Fu, B. J., Fan, Z. X., Wang, X. C. Zhang, Y. D., Halik, U.: Tree-ring based minimum
385 temperature reconstruction on the southeastern Tibetan Plateau, *Quat. Sci. Rev.*, 251, 106712.
386 <https://doi.org/10.1016/j.quascirev.2020.106712>, 2021

387 Keyimu, M., Wei, J. S., Zhang, Y. X., Zhang, S., Li, Z. S., Ma, K. M., Fu, B. J.: Climate signal shift under the influence of
388 prevailing climate warming – Evidence from *Quercus liaotungensis* on Dongling Mountain, Beijing, China,
389 *Dendrochronologia*, 60, 125683. <https://doi.org/10.1016/j.dendro.2020.125683>, 2020

390 Li, J. B., Shi, J. F., Zhang, D. D., Yang, B., Fang, K. Y. and Yue, P. H.: Moisture increase in response to high-altitude warming
391 evidenced by tree-rings on the southeastern Tibetan Plateau, *Clim. Dyn.*, 48, 649–660. [https://doi.org/10.1007/s00382-016-](https://doi.org/10.1007/s00382-016-3101-z)
392 [3101-z](https://doi.org/10.1007/s00382-016-3101-z), 2017

393 Li, T., Li, J.B.: A 564-year annual minimum temperature reconstruction for the east central Tibetan Plateau from tree rings,
394 *Glob. Planet. Change*, 157, 165-173. <https://doi.org/10.1016/j.gloplacha.2017.08.018>, 2017.

395 Li, Z. S., Zhang, Q. B. and Ma, K. P.: Tree-ring reconstruction of summer temperature for A.D. 1475–2003 in the central
396 Hengduan Mountains, northwestern Yunnan, China, *Clim. Change*, 110(1-2), 455-467, [https://doi.org/10.1007/s10584-011-](https://doi.org/10.1007/s10584-011-0111-z)
397 [0111-z](https://doi.org/10.1007/s10584-011-0111-z), 2011

398 Linderholm, H. W., Chen, D.: Central Scandinavian winter precipitation variability during the past five centuries reconstructed
399 from *Pinus sylvestris* tree rings, *Boreas*, 34, 43–52, <https://doi.org/10.1080/03009480510012845>, 2005

400 Michaelsen, J.: Crossevalidation in statistical climate forecast models, *J Clim. App. Meteorol.*, 26, 1589-1600, 1987

401 R: A language and environment for statistical computing. R Foundation for Statistical Computing, Vienna, Austria. URL
402 <https://www.R-project.org/>, 2020

403 Oquist, G., Huner, N. P.: Photosynthesis of overwintering evergreen plants, *Annu. Rev. Plant Biol.*, 54, 329–355.
404 <https://doi.org/10.1146/annurev.arplant.54.072402.115741>, 2003

405 Prats, K. A., Brodersen, C. R.: Seasonal coordination of leaf hydraulics and gas exchange in a wintergreen fern, *AoB Plants*,
406 12(6), 1–13. <https://doi.org/10.1093/aobpla/plaa048>, 2020

407 Pederson, N., Cook, E. R., Jacoby, G. C., Peteet, D. M., Griffin, K. L.: The influence of winter temperatures on the annual
408 radial growth of six northern range margin tree species, *Dendrochronologia*, 22 (1), 7–29.
409 <https://doi.org/10.1016/j.dendro.2004.09.005>, 2004

410 Rangwala, I., Miller, J. R. and Xu, M.: Warming in the Tibetan Plateau: Possible influences of the changes in surface water
411 vapor, *Geophys. Res. Lett.*, 36, L06703, <https://doi.org/10.1029/2009GL037245>, 2009

412 Schenk, H. J., & Jackson, R. B.: The global biogeography of roots. *Ecol. Monogr.*, 72, 311–328. [https://doi.org/10.1890/0012-9615\(2002\)072\[0311:TGBOR\]2.0.CO;2](https://doi.org/10.1890/0012-9615(2002)072[0311:TGBOR]2.0.CO;2), 2002

414 Schneider, L., Smerdon, J. E., Büntgen, U., Wilson, R. J. S., Myglan, V. S., Kirilyanov, A. V. and Esper, J.: Revising mid-
415 latitude summer temperatures back to AD 600 based on a wood density network, *Geophys. Res. Lett.*, 42, 4556–4562.
416 <https://doi.org/10.1002/2015GL063956>, 2015

417 Shi, C. M., Sun, C., Wu, G. C., Wu, X. C., Chen, D. L., Masson-Delmotte, V., Li, J. P., Xue, J. Q., Li, Z. S., Ji, D. Y., Zhang,
418 J., Fan, Z. X., Shen, M. G., Shu, L. F., Ciais, P.: Summer temperature over Tibetan Plateau modulated by Atlantic multi-
419 decadal variability, *J. Clim.*, 32, 4055–4067. <https://doi.org/10.1175/JCLI-D-17-0858.1>, 2019

420 Shi, S. Y., Li, J. B., Shi, J. F., Zhao, Y. S. and Huang, G.: Three centuries of winter temperature change on the southeastern
421 Tibetan plateau and its relationship with the Atlantic Multidecadal Oscillation, *Clim. Dyn.*, 49, 1305–1319.
422 <https://doi.org/10.1007/s00382-016-3381-3>, 2017

423 Sommerfeld, R. A., Mosier, A. R., Musselman, R. C.: CO₂, CH₄ and N₂O flux through a Wyoming snowpack and implications
424 for global budget, *Nature*, 361, 140–142, <https://doi.org/10.1038/361140a0>, 1993

425 Stadler, D., Wunderli, H., Auckenthaler, A., Fluhler, H.: Measurement of frost induced snowmelt runoff in a forest soil, *Hydrol.*
426 *Process.*, 10, 1293–1304, [https://doi.org/10.1002/\(SICI\)1099-1085\(199610\)10:10<1293::AID-HYP461>3.0.CO;2-I](https://doi.org/10.1002/(SICI)1099-1085(199610)10:10<1293::AID-HYP461>3.0.CO;2-I), 1996

427 Wang, J. L., Yang, B., Ljungqvist, F. C.: A millennial summer temperature reconstruction for the eastern Tibetan Plateau from
428 tree-ring width, *J. Clim.*, 28(13), 5289–5304. <https://doi.org/10.1175/JCLI-D-14-00738.1>, 2015

429 Wernicke, J., Griessinger, J., Hochreuther, P., Bräuning, A.: Variability of summer humidity during the past 800 years on the
430 eastern Tibetan plateau inferred from $\delta^{18}\text{O}$ of tree-ring cellulose. *Clim. Past*, 10(4), 3327–3356. <https://doi.org/10.5194/cp-11-327-2015>. 2015

432 Wigley, T. M., Briffa, K. R., and Jones, P. D.: On the average value of correlated time series, with applications in
433 dendroclimatology and hydrometeorology, *J. Clim. Appl. Meteorol.*, 23, 201–213, [https://doi.org/10.1175/1520-0450\(1984\)0232.0.CO;2](https://doi.org/10.1175/1520-0450(1984)0232.0.CO;2), 1984

435 Wilson, R., Anchukaitis, K., Briffa, K. R., Büntgen, U., Cook, E., D'Arrigo, R., Davi, N., Esper, J., Frank, D., Gunnarson, B.,
436 Hegerl, G., Helama, S., Klesse, S., Krusic, P.J., Linderholm, H.W., Myglan, V., Osborn, T.J., Rydval, M., Schneider, L.,
437 Schurer, A., Wiles, G., Zhang, P. and Zorita, E.: Last millennium northern hemisphere summer temperatures from tree rings:
438 Part I: the long-term context, *Quat. Sci. Rev.*, 134, 1-18. <https://doi.org/10.1016/j.quascirev.2015.12.00>, 2016

439 Wu, G., Duan, A., Liu, Y., Mao, J., Ren, R., Bao, Q., He, B., Liu, B. and Hu, W.: Tibetan Plateau climate dynamics: recent
440 research progress and outlook, *Natl. Sci. Rev.*, 2, 100–116, <https://doi.org/10.1093/nsr/nwu045>, 2015

441 Wu, X. C., Li, X. Y., Liu, H. Y., Ciais, P., Li, Y. Q., Xu, C. Y., Babst, F., Guo, W. C., Hao, B. Y., Wang, P., Huang, Y. M.,
442 Liu, S. M., Tian, Y. H., He, B. and Zhang, C. C.: Uneven winter snow influence on tree growth across temperate China, *Glob.*
443 *Change Biol.*, 25, 144–154. <https://doi.org/10.1111/gcb.14464>, 2019

444 Yan, L. and Liu, X.: Has climatic warming over the Tibetan Plateau paused or continued in recent years? *J. Earth Ocean Atmos.*
445 *Sci.*, 1, 13–28, 2014

446 Yang, B., Qin, C., Wang, J., He, M., Melvin, T. M., Osborn, T. J.: A 3,500-year tree-ring record of annual precipitation on the
447 northeastern Tibetan Plateau, *Proc. Natl. Acad. Sci. U. S. A.*, 111(8), 2903-2908. <https://doi.org/10.1073/pnas.1319238111>,
448 2014

449 Zhang, Q. B., Evans, M. N., Lyu, L. X.: Moisture dipole over the Tibetan Plateau during the past five and a half centuries, *Nat.*
450 *Commun.*, 6, 8062. <https://doi.org/10.1038/ncomms9062>, 2015

451 Zhu, H. F., Huang, R., Asad, F., Liang, E. Y., Bräuning, A., Zhang, X. Z., Dawadi, B., Man, W. M., Griessinger, J.: Unexpected
452 climate variability inferred from a 380-year tree-ring earlywood oxygen isotope record in the Karakoram, Northern Pakistan,
453 *Clim. Dyn.*, <https://doi.org/10.1007/s00382-021-05736-6>, 2021